

# STUDY OF A TRIAXIAL SPECIMEN AND A REVIEW FOR THE TRIAXIAL MACHINES

PhD Student Eng. Comanici A. M., Prof. Dr. Eng. Goanta V., Prof. Dr. Eng. Barsanescu P. D.  
Faculty of Mechanical Engineering – “Gheorghe Asachi” Technical University of Iași, Iasi, Romania  
E-mail: ana.comanici@yahoo.com, vgoanta@tuiasi.ro, paulbarsanescu@yahoo.com

**Abstract:** The paper presents a review of the most important triaxial testing machines and triaxial specimens from literature. It also includes a finite element analysis of a triaxial specimen. The main feature that is studied refers to the geometry of the specimen so that it is obtained a state of stress as favourable as possible for the fracture to occur.

**KEYWORDS:** TRIAXIAL TENSILE TEST, STRESS STATE, FINITE ELEMENT ANALYSIS, SPECIMEN

## 1. Introduction

In engineering applications, ductile behavior of solid materials is preferred [2]. Reaching the limit stress state of a material signifies in the broad sense, lost of its load bearing capacity. It can occur for example by fracture at brittle materials or appearance of the yield field for materials that shows ductile behavior. Predicting the limit stress state of the material subjected to multiaxial stress is very difficult. Ductile materials under triaxial tests are still insufficiently investigated, but the existing results describe two phenomena:

- failure cannot take place under the equi-triaxial stress compression state [4];
- failure of the specimen under triaxial tensile tension is always having a fragile character [3].

### 2.1 Triaxial testing machines

These machines are based on hydraulic actuators to apply forces to the tested specimens. Active-controlled hydraulic system configurations allows variation ratio of forces acting on the specimen on the desired direction so as to obtain a complete failure envelope.

*Calloch* and *Marquis* describe their machine as being able to load a cube of material in tension or compression along three perpendicular directions. The machine has been developed by LMT-Cachan and Schenck AG, Darmstadt, Germany and it has six servo hydraulic actuators that actually apply the loads up to 250kN. In front of each actuator there are additional hydrostatic bearings and along each axis the two actuators are coupled together to maintain the loadings. The central point of the specimen is motionless thus avoiding coupling between the different axes of the specimen [1].

A complex electromechanical system for testing, able to apply any combination of loads: tension and / or compression on the three mutual orthogonal axes on a cruciform specimen with its central area thickness reduced compared to the thickness of the arms was designed, manufactured, assembled and evaluated by *Welsh* and *Adams* [8]. *Welsh* triaxial machine is formed from three subsystems: the reaction frame, the test fixture and the computer control system. The main structural component is the reaction frame which provides precise alignment of the six force actuators, of the test fixture in relation with the force actuators and a surface that holds the test fixture. The machine was designed for maximum forces of  $\pm 133$  kN, but the six force actuators can generate forces up to  $\pm 94$  kN because of undersized drive motors [6].

A similar system was developed at the University of Castilla – La Mancha – Ciudad Real, Spain [9]. There, the machine has six actuators, six pneumatic grips and six electric gear motor for each actuator. In order to control the displacement or the loads applied to the specimen, the machine has specific software. The measurement of the loads is made with loading cells and the displacements of the actuator are regulated by encoder. The machine has a maximum load of 50 kN/axis and 50 mm/actuator displacement.

The University of Sheffield from United Kingdom also has a triaxial testing machine [5]. Their *mac<sup>2T</sup>* machine was designed to satisfy some of the following criteria: multiaxial compression of 100 mm cubic specimens up to 400 MPa at any Lode angle, ability

to test in the post-peak range because by monitoring post-peak response the information about ductility and fracture can be obtained, multiaxial compression at temperatures up to 300°C, complex multi stage experiments following arbitrary pre-programmed loading paths with simultaneous temperature cycling, to minimize the friction on the platen specimen interface, to ensure that the three stresses are delivered centrally on the six faces of the specimen [5]. The load in *mac<sup>2T</sup>* is delivered by three 4 MN hydraulic actuators installed in independent, diagonally interlaced loading frames.

### 3.2 Triaxial specimens

*Calloch* specimen has the form of a cube. The specimen was subjected to a heat treatment of 1 hour at 1050°C and in order to ensure initial isotropy of the material the specimen went through a process of annealing in water. This cube was made of 316 austenitic stainless steel, with an edge of 80 mm. Each face of the cube has drilled four 3 mm diameter holes and saw cuttings, which results in a center small cube with 9 mm edge [1].

*Welsh* specimen is cruciform made out of composite materials with its central area thickness reduced compared to the thickness of the arms [7]. The triaxial specimen has an extension glued on third direction which makes the results difficult to validate. It is 161 mm long across posing 24.8 mm wide loading arms, each of which contain two 4.76 mm diameter holes used to align each set of wedge grips assume a specimen thickness of 4.06 mm and a gage section thickness-taper fillet radius of 12.7 mm [6].

### 4.3 Geometric parameters of triaxial specimen

The specimens used for spatial state of stress (Fig.1) present some important features that have to be taken into consideration when a finite element analysis is going to be made or if the actual experiments take place.

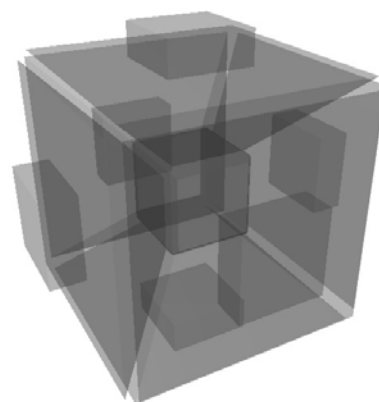


Fig. 1 Triaxial specimen – spatial view

Some of those characteristics are: the existence of stress concentrators in the section of the specimen due to how the connection is made (corner region or plain region), a surface where the triaxial testing machine applies the force, a intermediary segment of the specimen which submit to the stress but it only

makes the connection between the surface and the center of specimen. Another important aspect is the calculus method to determinate the stresses from the forces applied on the central cube. For this paper the specimen was considered cubic recreating the Calloch specimen with an edge of 80 mm, 3 mm diameter holes and cuttings, 400 mm<sup>2</sup> the surface to apply the loadings (Fig. 2).

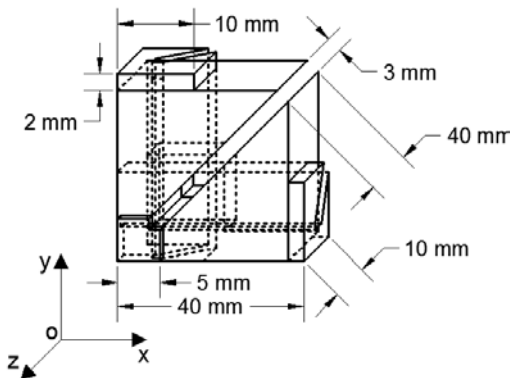


Fig. 2 The scheme of one eighth of the specimen and dimensions of elements

5. Finite element analysis

The specimen was tested for triaxial tension with a load of 12 MPa distributed on a surface of 109.3 mm<sup>2</sup> to determine the evolution in plasticity domain. We analyzed one eighth of the initial cube (Fig. 3) due to geometry and loadings symmetry conditions.

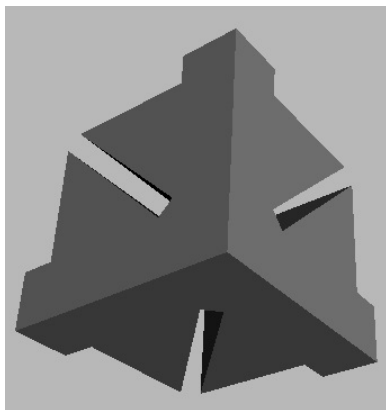


Fig. 3 One eighth of the specimen

Boundary conditions imposed to the specimen: no translation on perpendicular plans in relation with symmetry ones, no rotation on the symmetry plans (Fig. 4).

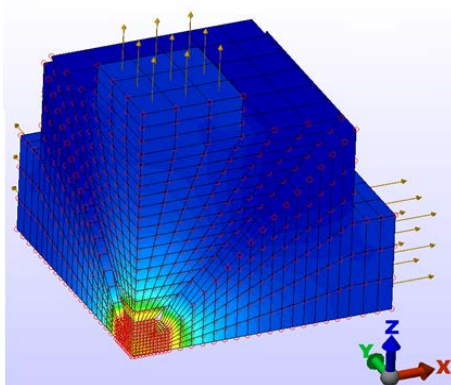


Fig. 4 Loading and symmetry conditions for the specimen

The material adopted to perform FEA was AISI 1010 Steel from program's library that has strain hardening modulus of 302.248 MPa, yield strength of 305 MPa and Young modulus of 205000 MPa. Simulation was made in ALGOR program, analysis type

being "MES with Nonlinear Material Models" and the elements type was "brick". FEA were conducted on two versions of the specimen as they are presented in the following figures.

This study is preliminary in order to validate the finite element analysis of the triaxial specimen and to achieve an optimisation of the geometry so that a state of stress as favourable as possible is obtained. In this paper we have two geometries of the specimen that come from the execution of the canals. The canals diameter is 3 mm on both cases, but first geometry has a canal made with a cutter with sharp tip referred as geometry 1 and the second geometry is made with a cutter without the angle tip referred as geometry 2. Requirements in composed solicitations are high stress state in failure volume, more uniform stress distribution and stress ratio to be constant till failure.

2.1 Geometry 1

The specimen's canals have been extruded using a cutter with a sharp tip that has an angle of 90° so from a initial cube we would have the gripping parts with a trapezoidal shape, canals of 3 mm and in center would be a full cube that has a side of 10 mm.

Fig. 5, Fig. 6 and Fig 7 are the maps of the stresses and strains in the specimen in the plastic-elastic simulation.

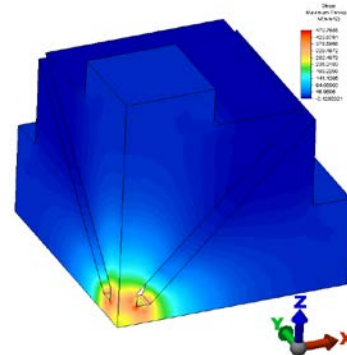


Fig.5 Maximum principal stress distribution

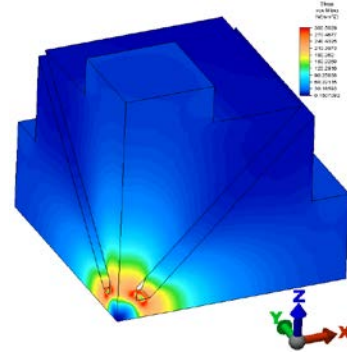


Fig.6 von Mises stress distribution

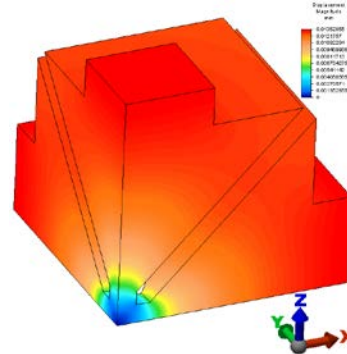


Fig.7 Displacement magnitude evolution

Maximum principal stress and von Mises stress have a distribution more constant and higher value at the periphery cube which means that the objective of having higher stresses in failure volume is achieved. Even though the maximum principal stresses has a higher value up to 470MPa, the von Mises stress is more concentrated with a high end value of 300MPa.

Fig. 8, Fig. 9 and Fig. 10 are the maps for the middle cube of 10mm that was mentioned before. Here we can observe better the stress and displacement that takes place after the loading takes place.

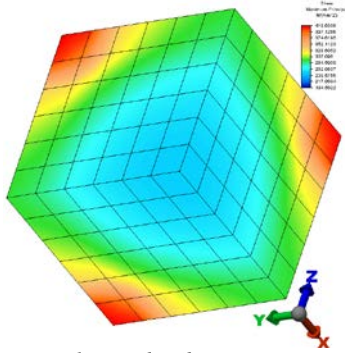


Fig.8 Maximum principal stress distribution

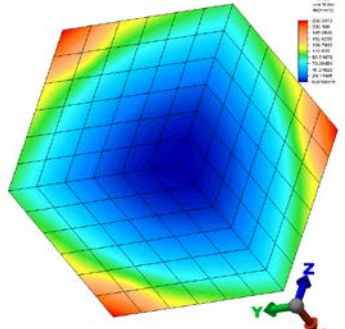


Fig.9 von Mises stress distribution

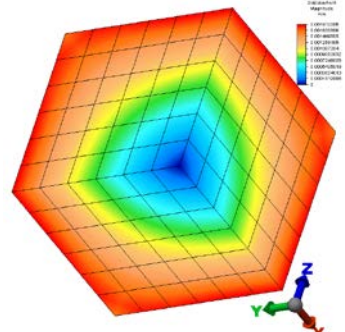


Fig.10 Displacement magnitude evolution

### 2.2 Geometry 2

On the second geometry that has been studied the canals were made with a disk in order to not have any angles in the middle cube.

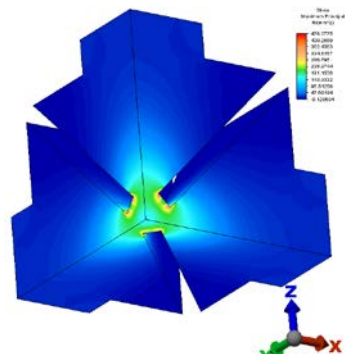


Fig.11 Maximum principal stress distribution

The failure will appear at the corners of the periphery cube and will advance towards interior. From Fig. 11 to Fig. 16 it is seen the symmetry of both the stresses and the deformations in relation to planes of symmetry. As a result, the symmetrical loading and support conditions are well defined. On the other hand, it appears that the movement pattern (Fig. 14, 15 and 16) confirms the correct application of boundary condition.

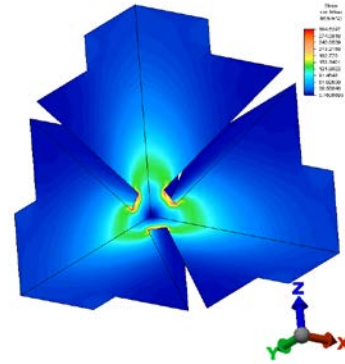


Fig.12 von Mises stress distribution

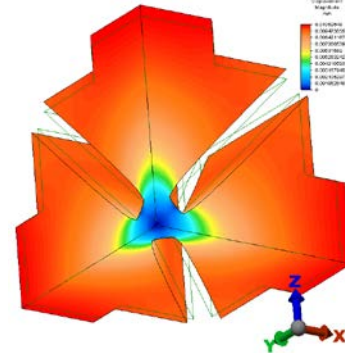


Fig.13 Displacement magnitude evolution

In the center of the specimen *von Mises* stresses are equal to zero and the value is obtained in triaxial state of stress using Eq. 2.

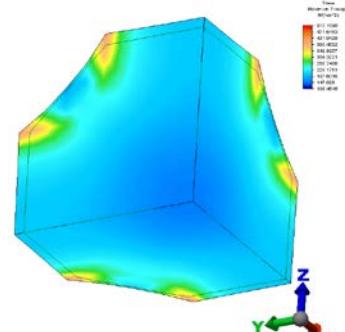


Fig.14 Maximum principal stress distribution

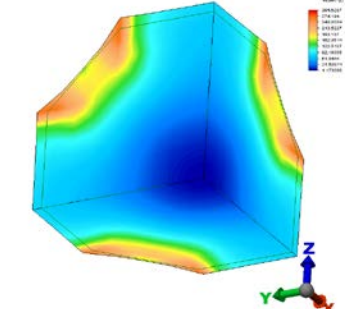


Fig.15 von Mises stress distribution

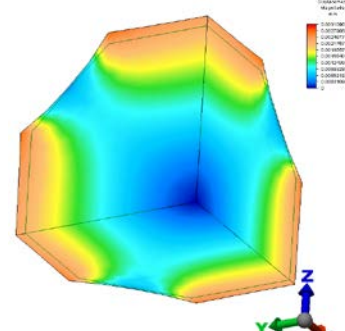


Fig.16 Displacement magnitude evolution

### 3. Results and discussion

Maximum principal stress has higher values in geometry 1 compared with geometry 2, case which is also seen for *von Mises* stress (Fig. 17 and Fig. 18).

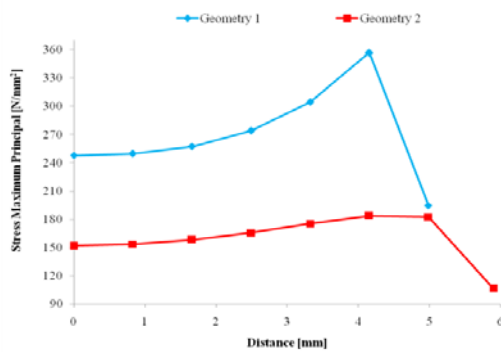


Fig. 17 Graphic representation of maximum principal stress

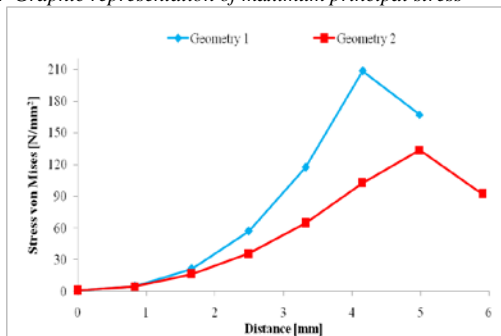


Fig. 18 Graphic representation for von Mises stress

According to actual failure theories the yielding stress can be wrote:

i. Tresca theory:

$$(1) \sigma_y = \sigma_1 - \sigma_3$$

ii. von Mises theory:

$$(2) (\sigma_1 - \sigma_2)^2 + (\sigma_2 - \sigma_3)^2 + (\sigma_3 - \sigma_1)^2 = 2\sigma_y^2$$

iii. in case of hydrostatic stress:

$$(3) \sigma_1 = \sigma_2 = \sigma_3$$

hence the Eq. 1, respectively Eq. 2 will become:

$$(4) \sigma_1 = 0 \text{ where } \sigma_1, \sigma_2, \text{ and } \sigma_3 \text{ are the maximum principal stresses and } \sigma_y \text{ is the yielding stress.}$$

Due to Eq. 4 it shows that the well known failure theories can not be applied on the triaxial state of stress as yielding stress will be all the time at a higher value then zero in order to have the yielding process start within the specimen. It is important to specify that von Mises stress is dangerous even if its value is zero or almost zero in all specimen volume (Fig. 18).

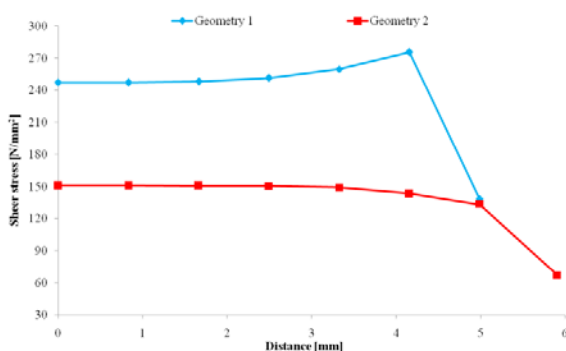


Fig. 19 Graphic representation of shear stress

The shear stress describes the fracture zone (Fig. 19) and the displacements magnitude represents the absolute value of the displacements (strain) of the specimen (Fig. 20).

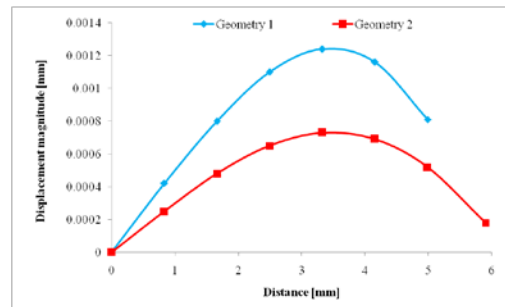


Fig.20 Graphic representation of displacement magnitude

### 4. Conclusions

One of the hypothesis of this paper was the schematization of the stress-strain curve using two lines that give the elasticity modulus (*Young's* modulus) and plasticity modulus.

Because the triaxial machine are very difficult to make and requires a dedicated data system and considerable resources, with the finite element analysis we want to optimize the shape of the specimen, to obtain a more favorable state of stress or closer to the ideal. This study was made to emphasize the need of a new equi-triaxial state of stress theory because even if *von Mises* stress is zero in the center of the specimen, this happens due to the fact that *von Mises* theory can not be applied for equi-triaxial state of stress and does not mean that the state of stress is not dangerous.

It was obtained a relatively uniform state of stress, with higher value in geometry 1 case, both for shear stress and maximum principal stress. Those high stresses are describing the failure section and the shear stress predicts fracture mode and so it is recommended the use of geometry 1.

### 5. Acknowledgement

This work was supported by the strategic grant POSDRU/159/1.5/S/133652, co-financed by the European Social Fund within the Sectorial Operational Program Human Resources Development 2007 – 2013.

### 6. References

- [1] Calloch, S., D. Marquis: Triaxial tension compression tests for multiaxial cyclic plasticity, *International Journal of Plasticity* 15 (1999), pp. 521-549 (1998).
- [2] Christensen R.M.: Failure Theory for Materials Science and Engineering, Chapter VII, The Ductile/Brittle Transition, Gaging Ductility Levels, [http://www.failurecriteria.com/Media/Ductile Brittle Transition Gaging Ductility Levels.pdf](http://www.failurecriteria.com/Media/Ductile%20Brittle%20Transition%20Gaging%20Ductility%20Levels.pdf) Accessed 15 September 2013.
- [3] Christensen R.M.: The Theory of Materials Failure. Oxford Univ. Press, ISBN 978-0-19-966211-1, 2013.
- [4] Yu Mao-hong: Advances in strength theories for materials under complex stress state in the 20th Century. *Appl. Mech. Rev.* 55, no 3, 2002, pp. 169-218.
- [5] Petkovski, M., R.S. Crouch, P. Waldron: Apparatus for Testing Concrete under Multiaxial Compression at Elevated Temperature (mac<sup>2T</sup>), *Experimental Mechanics* (2006), 46:387–398.
- [6] Welsh J.S., D.F. Adams: Development of a True Triaxial Testing Facility for Composite Materials, *Multiaxial Fatigue and Deformation: Testing and Prediction*, ASTM STP 1387, S. Kalluri and P.J. Bonacuse, Eds., American Society for Testing and Materials, West Conshohocken, PA, 2000, pp 423-437.
- [7] J.S. Welsh and D.F. Adams: Development of an Electromechanical Triaxial Test Facility for Composite Materials, *Experimental Mechanics* (2000); 40(3): 312-320.
- [8] J.S. Welsh, J.S. Mayes, and A. Biskner: 2-D biaxial testing and failure prediction of IM77/977-2 carbon/epoxy quasi-isotropic laminates, *Composite Structures* (2006); 75(1-4): 60-66.
- [9] M.C. Serna Moreno, J.L. Martínez Vicente, J.J. López Cela: Failure strain and stress fields of a chopped glass-reinforced polyester under biaxial loading, *Composite Structures* 103 (2013), pp.27–33.